medRxiv preprint doi: https://doi.org/10.1101/2021.08.31.21262868; this version posted July 15, 2022. The copyright holder for this preprint (which was not certified by peer review) is the author/funder, who has granted medRxiv a license to display the preprint in perpetuity. It is made available under a CC-BY-NC-ND 4.0 International license .

Optimal and worst testing strategies for COVID-19

Onishi Tatsuki[a,b,c], Honda Naoki[d,e,f]†, Yasunobu Igarashi[g,h] *

[a] Department of Pharmacoepidemiology, Graduate School of Medicine and Public Health, Kyoto University, Yoshidakonoecho, Sakyo, Kyoto, Japan

[b] Department of Anesthesiology and Pain Clinic, Juntendo University Shizuoka Hospital, Izunokuni, Shizuoka, Japan

[c] Department of Anaesthesiology, Tokyo Metropolitan Bokutoh Hospital, Kotobashi, Sumida, Tokyo, Japan

[d] Laboratory for Data-driven Biology, Graduate School of Integrated Sciences for Life, Hiroshima University, Higashihiroshima, Hiroshima, Japan

[e] Theoretical Biology Research Group, Exploratory Research Center on Life and Living Systems (ExCELLS), National Institutes of Natural Sciences, Okazaki, Aichi, Japan

[f] Laboratory of Theoretical Biology, Graduate School of Biostudies, Kyoto University, Yoshidakonoecho, Sakyo, Kyoto, Japan

[g] E2D3.org, izumi-cho, Kokubunji, Tokyo, Japan

[h] Center for Research on Assistive Technology for Building a New Community, Nagoya Institute of Technology, Nagoya, Aichi, Japan

* Corresponding author
Yasunobu Igarashi
Center for Research on Assistive Technology for Building a New Community, Nagoya Institute of Technology
Gokiso-cho, Showa-ku, Nagoya, Aichi, 466-8555 Japan
Tel.: +81-52-735-5334
E-mail: yasunobu.igarashi@gmail.com

† Co-corresponding author
Honda Naoki
Laboratory for Data-driven Biology, Graduate School of Integrated Sciences for Life, Hiroshima University, 1-3-2 Kagamiyama, Higashi-Hiroshima City, Hiroshima, 739-8511 Japan
Tel.: +81-82-424-7336
E-mail: nhonda@hiroshima-u.ac.jp

NOTE: This preprint reports new research that has not been certified by peer review and should not be used to guide clinical practice.

medRxiv preprint doi: https://doi.org/10.1101/2021.08.31.21262868; this version posted July 15, 2022. The copyright holder for this preprint (which was not certified by peer review) is the author/funder, who has granted medRxiv a license to display the preprint in perpetuity. It is made available under a CC-BY-NC-ND 4.0 International license .

Abstract

Background

During the last three years of fighting COVID-19, governments have been seeking optimal solutions to minimize the negative impacts on societies. They actively used mathematical models such as the susceptible, infectious, exposed, recovered, and dead (SEIRD) model to predict the spread of infection. However, in the end, all governments had difficulty figuring out how to adopt testing strategies.

Methods

In this study, we developed a testing-SEIRD model, which incorporates testing strategy and testing characteristics. In this model, people who are tested positive are admitted to the hospital within the capacity and medical resources. Through simulations, we examined the infection spread depending on the balance between follow-up testing and mass testing, which test people closely contacted with infected persons and people with symptoms, respectively.

Results

We showed that there are optimal and worst combinations of the follow-up and mass testing. These strategies are subject to total resources and cost ratio of testing costs. We also found that these combinations provide an all-or-nothing response for whether the spread of infection expands or extinguishes.

Conclusions

While this model alerts us to the existence of a worst testing strategy, it also reveals that an optimal testing strategy can lead to infection containment. Therefore, the testing-SEIRD model is useful in making decisions on testing strategies for the emerging infectious disease outbreaks.

medRxiv preprint doi: https://doi.org/10.1101/2021.08.31.21262868; this version posted July 15, 2022. The copyright holder for this preprint (which was not certified by peer review) is the author/funder, who has granted medRxiv a license to display the preprint in perpetuity. It is made available under a CC-BY-NC-ND 4.0 International license .

Introduction

Coronavirus disease 2019 (COVID-19) emerged in Wuhan, China as global healthcare concern [1,2]. Due to its high transmission ability via aerosol, and to lack of a specific treatment in the early stage of the COVID-19 Alpha variant pandemic, 5.5 million people have been infected, and 350,000 people have died by April 2020 [3]. Medical resource in hospitals is primarily consumed by treatments for COVID-19 patients [1,2]. As of April 2020, approximately 10% of hospital beds, or 10-20% of ICU beds are occupied with COVID-19 care [3–5]. Moreover, from May 2020, the COVID-19 Beta variant emerged. Every time a new variant of concern (VOC) emerges, such as the Beta, Gamma, Delta and Omicron variant, society requires an update of knowledge about VOC [6–8].

To minimize the number of deaths, society should be aware of the advantages and disadvantages of testing for COVID-19 [9]. From a perspective of individuals, testing has advantages so that asymptomatic infected individuals can be detected and prepared for symptomatic treatment, whereas from a perspective of society, testing prevents secondary infections, expecting the reduction of the number of deaths [10–12]. On the other hand, testing has disadvantages especially at the initial pandemic stage as seen in the Alpha variant pandemic in April 2020, in which no specific treatment was established and testing characteristics, i.e., sensitivity and specificity, are unknown. From a perspective of individuals, the result of testing does not change medical care because of no specific treatment, whereas from a perspective of society, testing is done aimlessly and whether testing results should be trusted was uncertain, resulting in waste of medical and human resources. Therefore, in every early stage of every newly emerging VOC, policymakers should decide the volume of testing with knowledge of the testing characteristics.

There was a controversy about the testing policies to minimize the number of deaths in the early stage of the COVID-19 Alpha variant pandemic [7,10,11,13,15–20]. That controversy was between two extreme policies to balance the medical supply and demand: “mass-testing policy” and “no-testing policy” [21]. The mass-testing policy claims that all people must be tested for public health, regardless of the symptoms [22–24]. The mass-testing policy assumes that testing and hospitalization of asymptomatic patient is important to reduce the total number of deaths even in the absence of the specific treatment. Contrary to the mass-testing policy, no-testing policy claims that testing should be limited to symptomatic patient [21]. The no-testing policy assumes that asymptomatic patient cannot expect a benefit from mass-testing in the absence of a specific treatment. Although there is discordance in these two policies with different assumptions, these two policies agree with testing on people with symptoms. They disagree on the extent of the asymptomatic population tested.

What is the most practical testing policy to minimize the number of deaths? The testing strategies for people without symptoms have two options: follow-up testing-dominant strategy that follows and tests the exposed population and mass-testing-dominant strategy that randomly tests the infected population. There remains a problem that it is uncertain to what extent follow-up testing and mass-testing for asymptomatic

medRxiv preprint doi: https://doi.org/10.1101/2021.08.31.21262868; this version posted July 15, 2022. The copyright holder for this preprint (which was not certified by peer review) is the author/funder, who has granted medRxiv a license to display the preprint in perpetuity. It is made available under a CC-BY-NC-ND 4.0 International license .

populations will affect the number of deaths and lead to the optimal and the worst outcomes especially in early stage of emerging VOC in future [7,10,11,13,15–20].

In this paper, we developed a testing-SEIRD model, aiming to evaluate the testing strategy with a mixture of follow-up and mass-testing in terms of minimization of the number of deaths in the early stage of the newly emerging VOC. The testing-SEIRD model took account for testing characteristics, testing strategies, hospitalized subpopulation, and the amount of medical resources [25]. Using this model, we examined the worst and optimal testing strategy in the condition that medical resources are both infinite and finite. We then found that the optimal testing strategy largely depends on the cost ratio of mass-testing and follow-up testing. Thus, this study sheds light on how to minimize the number of deaths in the absence of specific treatment in the early stages of pandemic.

medRxiv preprint doi: https://doi.org/10.1101/2021.08.31.21262868; this version posted July 15, 2022. The copyright holder for this preprint (which was not certified by peer review) is the author/funder, who has granted medRxiv a license to display the preprint in perpetuity. It is made available under a CC-BY-NC-ND 4.0 International license .

Model

To examine the effect of testing on the infection population dynamics, we developed a new model by introducing a hospitalised subpopulation, testing strategy, and testing characteristics into the classical SEIRD model. In general, the SEIRD model is described by the subpopulation dynamics of susceptible, exposed, infectious, recovered, and dead people (Fig. 1A) as:

$$\frac{dS}{dt} = -\frac{bIS}{N}, \tag{2.1}$$

$$\frac{dE}{dt} = \frac{bIS}{N} - gE, \tag{2.2}$$

$$\frac{dI}{dt} = gE - (r + d)I, \tag{2.3}$$

$$\frac{dR}{dt} = rI, \tag{2.4}$$

$$\frac{dD}{dt} = dI, \tag{2.5}$$

where S, E, I, R, and D indicate the populations of susceptible, exposed, infectious, recovered, and dead people, respectively. N indicates the total population, that is, $N=S+E+I+R$. b indicates the exposure rate, which reflects the level of social activity; g, r, and d indicate the transition rates among the subpopulations. For this model, it is assumed that the recovered populations acquire permanent immunity, indicating that they will never be infected.

Regarding the testing-SEIRD model, we incorporated the testing characteristics and testing strategy into the classical SEIRD model by dividing the population into outside and inside of the hospitals (Fig. 1B). The dynamics of the population outside the hospitals are described by:

$$\frac{dS_o}{dt} = -\frac{bI_oS_o}{N_o} + uE_o - aS_h, \tag{2.6}$$

$$\frac{dE_o}{dt} = -\frac{bI_oS_o}{N_o} - (u + g)E_o - f(1 - Sp)E_oH(C - N_h), \tag{2.7}$$

$$\frac{dI_o}{dt} = gE_o - (r_o + d_o)I_o - mSeI_oH(C - N_h), \tag{2.8}$$

$$\frac{dR_o}{dt} = r_oI_o, \tag{2.9}$$

$$\frac{dD_o}{dt} = d_oI_o, \tag{2.10}$$

and those inside hospitals were described by:

$$\frac{dS_h}{dt} = -\frac{bI_hS_h}{N_h} + uE_h + aS_h, \tag{2.11}$$

medRxiv preprint doi: https://doi.org/10.1101/2021.08.31.21262868; this version posted July 15, 2022. The copyright holder for this preprint (which was not certified by peer review) is the author/funder, who has granted medRxiv a license to display the preprint in perpetuity. It is made available under a CC-BY-NC-ND 4.0 International license .

$$\frac{dE_h}{dt} = \frac{bI_hS_h}{N_h} - (u+g)E_h + f(1-Sp)E_oH(C-N_h), \tag{2.12}$$

$$\frac{dI_h}{dt} = gE_h - (r_h + d_h)I_h + mSeI_oH(C-N_h), \tag{2.13}$$

$$\frac{dR_h}{dt} = r_hI_h, \tag{2.14}$$

$$\frac{dD_h}{dt} = d_hI_h, \tag{2.15}$$

where X_o and X_h indicate each population outside and inside the hospitals ($X \in \{S, E, I, R, D, N\}$); N_o and N_h indicate the total populations outside and inside hospitals, respectively (i.e., $N_o=S_o+E_o+I_o+R_o+R_h$ and $N_h=S_h+E_h+I_h$); a indicates the rate of discharge of S_h from hospital to the outside; u and g indicate the non-infection and infection rates, respectively; C indicates the capacity of hospitals. We assumed that these parameters are determined by the nature of the disease; thus, they are independent of inside and outside hospitals. r_j and d_j ($j \in \{o, h\}$) indicate the recovery and death rates from infection, respectively, where $r_o < r_h$, and $d_h < d_o$; f and m indicate the rates of follow-up and mass-testing, corresponding to the extent to which health centers follow exposed populations and take-up infected populations having symptoms, respectively; Sp and Se indicate specificity and sensitivity, respectively, as testing characteristics. The model assumed that I contains a fixed proportion of symptomatic and asymptomatic individuals, and that symptomatic infected individuals receive mass-testing. The hospitalization capacity was introduced by the sigmoid function $H(x) = 1/(1+\exp(x))$. The parameter values and initial conditions are listed in Table 1 and discussed in the Materials and Methods section.

medRxiv preprint doi: https://doi.org/10.1101/2021.08.31.21262868; this version posted July 15, 2022. The copyright holder for this preprint (which was not certified by peer review) is the author/funder, who has granted medRxiv a license to display the preprint in perpetuity. It is made available under a CC-BY-NC-ND 4.0 International license .

Results

We first examine the basic behavior of the testing-SEIRD model by simulation as shown in Fig. 2. Similar to the classical SEIRD model, infection largely expanded, and the infectious population (I_h and I_o) transiently increased in response to the occurrence of infectious people. Susceptible populations (S_h and S_o) gradually decreased and shifted into recovered populations (R_h and R_o) through the exposed (E_h and E_o) and infectious (I_h and I_o) states. During this process, the number of dead cells increases gradually as shown in Fig. 2A. The hospitalized population increase, plateau at the capacity of hospitalizations within the period of infection overshoot, and decrease by the hospital discharge (Fig. 2B). The outside population decrease by hospitalizations through testing and switch to a constant decrease, whereas the hospitalized population reaches its capacity and increases by the hospital discharge (Fig. 2B). Moreover, the outside and hospitalized populations are divided into five types of populations (susceptible, exposed, infectious, recovered, and dead) (Fig. 2C and D). Daily reports of positive tests and deaths transiently increase with different peak timings, and the peak of positive tests precedes that of deaths (Fig. 2E). Reproduction numbers (see Materials and Methods) outside hospitals RN_o switch from greater than one to less than one around the peak timing of infectious populations outside (Fig. 2F). On the contrary, reproduction numbers inside hospitals RN_h are less than one. This indicates that the infectious population in hospitals increases owing to supply from the outside; however, it is not because of the infectious spread in hospitals. The testing-SEIRD model recapitulates basic infection dynamics of the total population as observed in the classical SEIRD model (Fig. 2A), and enables us to examine the effect of the testing strategy and testing characteristics with different populations inside and outside hospitals.

To investigate the impact of hospitalization capacity on infection dynamics, such as daily reports of positive tests, hospitalizations, and deaths, we simulate the testing-SEIRD model with various capacities (Fig. 3A to C). We observe that as the capacity increases, the maximum positive tests, maximum hospitalizations, and cumulative deaths linearly decrease, increase, and decrease, respectively, and they all plateau at approximately 30% capacity (Fig. 3D to F). We have also examined their peak timings and have observe that they change nonlinearly, with certain time window ranges (Fig. 3G–I). These results suggest that the change in capacity has a large effect on the level of spread of the disease; nonetheless, it has a small effect on timing.

To illustrate the impact of the testing strategy on infectious outcomes, we examined the cumulative deaths, maximum number of positive tests and hospitalizations, varying follow-up and mass-testing rates. The infectious spread shows an all-or-none response depending on the testing strategy (red and blue regions in Fig. 4). Sensitivity analyses confirmed that such a profile was robustly maintained independent of the model parameters (Fig. S1 and S2).

The number of cumulative deaths is almost constant with a small amount of both the follow-up and mass-testing (red region in upper panel of Fig. 4A); nonetheless, the combination of follow-up and mass-testing cooperatively suppresses the infectious spread (blue region in the upper panel of Fig. 4A). We also realize that the maximum number of hospitalizations is immediately saturated by either the follow-up or

medRxiv preprint doi: https://doi.org/10.1101/2021.08.31.21262868; this version posted July 15, 2022. The copyright holder for this preprint (which was not certified by peer review) is the author/funder, who has granted medRxiv a license to display the preprint in perpetuity. It is made available under a CC-BY-NC-ND 4.0 International license .

mass-testing because of the limited hospitalization capacity (upper panel in Fig. 4B). The maximum number of positive tests increases more efficiently with the follow-up testing rate compared to the mass-testing rate (upper panel in Fig. 4C).

Subsequently, realistic scenarios were considered by adapting the limited resource L. Practically, we cannot freely control the follow-up and mass-testing rates because of the limited medical resource for both the follow-up and mass-testing. Thus, it is necessary to determine the amount of resource allocated to the follow-up and mass-testing. Here, we consider all the possible decisions subject to the limited resource L as:

$$L = c_f f + c_m m, \tag{3.1}$$

where c_f and c_m indicate the costs for follow-up and mass-testing, respectively; f and m are reflected by the decisions on how much follow-up and mass-testing are conducted. Considering different L, c_f, and c_m, based on the disease, economic and technological situations of each country, we depicted three lines. The three colored lines in the heat maps correspond to a cost ratio of 1:10, 1:5, and 1:1 for follow-up and mass-testing, respectively (Fig. 4). Given the total amount of resources, we can choose the optimal testing strategy on the line represented by the equation (3.1). We observe that the worst decisions (i.e., the choice of f and m) drastically varied depending on the situation (lower panels of Fig. 4).

Regarding the high resource and low ratio of the cost of follow-up testing to that of the mass-testing cost, the number of cumulative deaths abruptly increases as the resource fraction of mass-testing exceeds 90% (green line in Fig. 4A). This indicates that the mass-testing dominant testing is the worst strategy for minimizing the cumulative deaths. On the other hand, considering low resource and high ratio of follow-up cost to mass-testing cost, the number of cumulative deaths abruptly decreases at the resource fraction of 20% to 30 % (blue line in Fig. 4A) assigned to mass-testing. Contrary to the previous case, this result suggests that follow-up-dominant testing is the worst strategy. Regarding the intermediate situation between the two cases above, the simulation showed a U-shape with the resource fraction assigned to mass-testing ranging from approximately 10 to 80 % (orange line in Fig. 4A). These results clearly suggested that both follow-up and mass-dominant testing are strategies to avoid, whereas the optimal strategy is a combination of the follow-up and mass-testing. The choice of f and m also changed in the profiles of maximum hospitalizations and positive reports (Fig. 4B and C). Taken together, the optimal strategy for each country/region should be sought with the resource considered.

Moreover, we examined how the three variables (i.e., the number of cumulative deaths, hospitalizations, and positive tests) are affected by the testing characteristics (i.e., sensitivity and specificity). We conducted sensitivity analyses for Se and Sp with values from zero to four with 0.01 increments. We obtained almost the same heatmaps in the sensitivity-specificity space although the heatmaps were inverted along the x-axis (Fig. 5). The equations (2.7, 2.8, 2.12, and 2.13) reveal that sensitivity and one-specificity essentially play the same roles in the follow-up and mass-testing. The sensitivity and specificity of the test are not modifiable, whereas the testing strategy can be arbitrary. If the sensitivity is low, an increase in the mass-testing rate can lead to the same infectious result with high sensitivity. On the contrary, if the specificity is low, a decrease in the follow-up testing rate can lead to the same infectious result with high

medRxiv preprint doi: https://doi.org/10.1101/2021.08.31.21262868; this version posted July 15, 2022. The copyright holder for this preprint (which was not certified by peer review) is the author/funder, who has granted medRxiv a license to display the preprint in perpetuity. It is made available under a CC-BY-NC-ND 4.0 International license .

specificity. Therefore, we must manage the optimal testing strategy based on the unmodifiable testing sensitivity and specificity.

We have investigated how the infection is expanded based on the testing strategy. However, this is the point of view of a perfect observer who knows the exact time course of the latent populations. Practically, we are unable to know all the model variables, such as exposed and infectious populations inside and outside hospitals; nonetheless, we can merely monitor positive reports by follow-up and mass-testing. In this study, we verify whether these two kinds of positive reports reflect the latent infectious population, which is the most resource-consuming and challenging social issue. Using regression analysis (see Materials and Methods), we demonstrate that latent infectious populations can be predicted from daily positive reports of follow-up and mass-testing (Fig. 6A to C). These results suggest that the infectious population is not simply proportional to the sum of positive reports of follow-up and mass-testing; nevertheless, they are proportional to their weighted sum (Fig. 6D). There are cases in which either weights can be negative, depending on the model parameters. We found that the weight for positive reports of follow-up testing was negative with high positive predictive values. This is because the negative weight of P_f acts in a repressive manner to estimate the latent number of infectious people, reflecting a low positive predictive value (Fig. 6D).

medRxiv preprint doi: https://doi.org/10.1101/2021.08.31.21262868; this version posted July 15, 2022. The copyright holder for this preprint (which was not certified by peer review) is the author/funder, who has granted medRxiv a license to display the preprint in perpetuity. It is made available under a CC-BY-NC-ND 4.0 International license .

Discussion

We develop a testing-SEIRD model to consider two discrete populations inside and outside hospitals, impact of testing strategy (follow-up testing [*f*], and mass-testing [*m*]), and testing characteristics (sensitivity [*Se*] and specificity [*Sp*]) on three variables (i.e., the number of maximum positive tests, maximum hospitalizations, and cumulative deaths (Fig. 1)). By simulating the model with parameters, which describe the early stage of the COVID-19 Alpha variant pandemic, we demonstrate that the optimal and the worst testing strategies are subject to limited medical resource (Fig. 4). In addition, we highlight the possibility that the infectious population can be predicted by a weighted sum of positive reports from follow-up and mass testing (Fig. 6).

Comparison with previous models

There are several models of infectious dynamics, such as SIR [26] SEIRD models, and their alternatives, which have been widely used for policy making through model simulation [1,27–34]. However, some of the previous models do not include the hospital compartment, [28,33,35–37] and other models, even with hospital compartments, do not consider the testing strategy and testing characteristics [30,38]. They cannot address how the testing strategy and testing characteristics affect the number of deaths. Consequently, we develop the testing-SEIRD model by introducing new factors: the hospital compartment, testing strategy, testing characteristics, and medical resource to the previous SEIRD model (Fig. 2-4). The testing-SEIRD model generalizes the classical SEIRD model, and it can be equivalent to the classical SEIRD model if the testing strategy is removed (f=0, m=0).

Model prediction

Our model has three advantages. First, the testing-SEIRD model provides the best testing strategy for situations. The model provides heatmaps of the number of the three variables in the space of the testing strategy (Fig. 4). These heatmaps indicate the best direction as shown in the blue region in Fig. 4. This corresponds to the settling of infections using the shortest path. Second, the testing-SEIRD model can predict the optimal and worst strategies, considering the limited medical resource and ratios for the testing costs (Fig. 4). Because the total medical resource and testing costs depend on countries, our model offers the best testing strategy unique to each country. Third, the testing-SEIRD model demonstrates that the latent number of infectious populations can be predicted from daily positive reports of the follow-up and mass-testing (Fig. 6).

Validity of model components

Here, we discuss the validity of the model components, which previous models do not have. First, we focus on the transition from E_o to E_h (Fig. 1). We assume that the hospitalization of the exposed population is induced by the follow-up testing. Populations that are just exposed before developing symptoms do not take

medRxiv preprint doi: https://doi.org/10.1101/2021.08.31.21262868; this version posted July 15, 2022. The copyright holder for this preprint (which was not certified by peer review) is the author/funder, who has granted medRxiv a license to display the preprint in perpetuity. It is made available under a CC-BY-NC-ND 4.0 International license .

the tests themselves. They test only when urged by the follow-up. Second, related to the transition from I_o to I_h, we assume that the hospitalizations of the infectious population are induced by the mass-testing, which is defined as a person with symptoms. Considering our model, we address the rate of mass-testing as a modifiable parameter because the rate depends on the volume of the tests, such as polymerase chain reaction (PCR) and the degree of social penalty if it is positive. Third, we consider the transition from E_o to S_o and E_h to S_h. Regarding our model, all the exposed populations are not necessarily infected and some return susceptible compared to the previous models which assume that all the exposed populations are destined to be infected [28,30,32,33,35–41]. Consistent with our model, it is well known that some exposed populations return to susceptible populations without developing symptoms. Finally, our model is not specific to the Alpha variant, but is applicable to other VOCs, because the assumptions mentioned above about exposure, infection and hospitalization processes are common in VOCs [8]. Taken together, new components introduced into the testing-SEIRD model not only are consistent with the previous simulation model, but also reflect and incorporate a practical point of view.

Validity of model parameters

We used parameters from the previous reports before the Beta variant appeared in South Africa in May 2020 [8] (Table 1) because the earlier reports are homogeneous Alpha variant data. After May 2020, the reports are an inhomogeneous mixture of multiple variants. We set sensitivity and specificity of testing to 0.7 and 0.7 accordingly and the results were robustly guaranteed by a sensitivity analysis (Fig. 4). As the incubation and infectious periods remain roughly stable in the VOCs, while the number of reproductions and mortality rates vary among variants [8,12,14]. The number of reproductions, reinfection [42] effects were robustly guaranteed by a sensitivity analysis of b and u (Fig. S1). Mortality was taken into account in the model with d_o and d_h and these values are sensitivity analyzed (Fig. S2). a or the rate of discharge from S_h was robustly guaranteed by a sensitivity analysis (Fig. S3). Although these values are based on the COVID-19 Alpha variant, our sensitivity analysis indicates that the testing-SEIRD robustly generated the optimal and worst testing strategy for other VOCs having different parameters.

Future studies

Considering the future perspectives of our model, first, our testing-SEIRD model simulates only a single peak time course of infection. However, we observed multiple peaks of COVID-19 infection in many countries [43]. To incorporate the multiple peaked dynamics, we must introduce the socio-psychological effects caused by policies such as lockdown and social distancing. Second, our model assumes that all the populations are homogeneous and do not address stratification based on attributes such as gender, age, social activities, and comorbidities [44,45]. A future study should consider this perspective. Finally, our model does not include the effects of vaccination. We are currently fighting the spread of COVID-19 using messenger RNA (mRNA) vaccines. It seems we are getting successful results; however, we do not know the

medRxiv preprint doi: https://doi.org/10.1101/2021.08.31.21262868; this version posted July 15, 2022. The copyright holder for this preprint (which was not certified by peer review) is the author/funder, who has granted medRxiv a license to display the preprint in perpetuity. It is made available under a CC-BY-NC-ND 4.0 International license .

duration of the effect of the vaccinations or acquired immunity and its effectiveness against VOCs [43,46,47]. Therefore, the tag-of-war model between vaccines and virus evolution remains elusive.

medRxiv preprint doi: https://doi.org/10.1101/2021.08.31.21262868; this version posted July 15, 2022. The copyright holder for this preprint (which was not certified by peer review) is the author/funder, who has granted medRxiv a license to display the preprint in perpetuity. It is made available under a CC-BY-NC-ND 4.0 International license .

Materials and Methods

Parameter set

The parameters and initial conditions of the simulation are listed in Table 1A. We used parameters based on the studies of the COVID-19 Alpha variant. The total population N was set to 1,000,000 according to the United Nations Statistical Papers: The World's Cities in 2018, which mentioned that one in five people worldwide lives in a city with more than one million inhabitants and the median value of inhabitants is between 500,000 and one million [48]. Sensitivity Se and specificity Sp were both set to 0.7, which correspond to those of the PCR for detecting COVID-19 (Table 1B) [28,39,49–51]. The values of b, g, r_h, r_o, and d_h are based on previous reports (Table 1C) [3,29–34,36–38,42]. The sum of u and g is the inverse of the incubation period during the exposed state, which is reported to be five days (Table 1C) [31–33,41,50]. The sum of r and d is the inverse of the infectious period during the infectious state, which is reported to be ten days (Table 1D) [31,32,35,50].

Definitions of reproduction numbers

Considering Fig. 2, we computed the time courses of reproduction numbers inside and outside hospitals: RN_h and RN_o.

$$RN_h = \frac{1}{r_h + d_h} \cdot \frac{bS_h}{S_h + E_h + I_h} \cdot \frac{g}{u + g}, \tag{5.1}$$

$$RN_o = \frac{1}{r_o + d_o} \cdot \frac{bS_o}{S_o + E_o + I_o + R_o + R_h} \cdot \frac{g}{u + g}. \tag{5.2}$$

Here, the first, second, and third factors in these equations indicate the average infectious period, infection rate, and probability that the exposed state transits to the infectious state, respectively. The reproduction number in the classical SEIRD model is defined in previous studies [1,27–34] as:

$$RN = \frac{1}{r + d} \cdot \frac{bS}{S + E + I + R}. \tag{5.3}$$

medRxiv preprint doi: https://doi.org/10.1101/2021.08.31.21262868; this version posted July 15, 2022. The copyright holder for this preprint (which was not certified by peer review) is the author/funder, who has granted medRxiv a license to display the preprint in perpetuity. It is made available under a CC-BY-NC-ND 4.0 International license .

Acknowledgments

We thank Tomohiko Takada M.D. (Ph.D.) and Yoshika Onishi M.D. (Ph.D.) for providing the basic concept of clinical NNT. We thank Yoshiaki Yamagishi M.D. (Ph.D.), Tomokazu Doi M.D. (Ph.D.), and Tatsuyoshi Ikenoue M.D. (Ph.D.) for polishing early manuscript. We also thank Prof. Hiroshi Nishiura for providing the fundamental knowledge of infectious disease modelling by organising a summer boot camp in 2014.

Funding

This study was partly supported by the Cooperative Study Program of Exploratory Research Centre on Life and Living Systems (ExCELLS) (program Nos.18-201, 19-102, and 19-202 to H.N.), a Grant-in-Aid for Transformative Research Areas (B) [grant number 21H05170], a Grant-in-Aid for Scientific Research (B) (21H03541 to H.N.) from the Japan Society for the Promotion of Science (JSPS).

Ethics

Any human or animal subjects are not involved in this manuscript.

Data Availability

All relevant data are within the study and its supporting information files.

Code Availability

All codes to reproduce the results of this study are hosted in Github at https://github.com/bougtoir/testing-SEIRD.

Author Contributions

O.T. and Y.I. conceived of the initial ideas. O.T. developed and implemented the method, processed, and analysed the data, and wrote the initial draft of the manuscript. H.N. edited the initial draft of the manuscript and reviewed the method. Y.I. supervised the project. All authors contributed to the final writing of the manuscript.

Competing Interests

The authors declare no competing interests.

medRxiv preprint doi: https://doi.org/10.1101/2021.08.31.21262868; this version posted July 15, 2022. The copyright holder for this preprint (which was not certified by peer review) is the author/funder, who has granted medRxiv a license to display the preprint in perpetuity. It is made available under a CC-BY-NC-ND 4.0 International license .

References

1. Shereen MA, Khan S, Kazmi A, Bashir N, Siddique R. 2020 COVID-19 infection: Origin, transmission, and characteristics of human coronaviruses. *Journal of Advanced Research* **24**, 91–98. (doi:10.1016/j.jare.2020.03.005)
2. Kolifarhood G, Aghaali M, Saadati HM, Taherpour N, Rahimi S, Izadi N, Saeed S, Nazari H. 2020 Epidemiological and Clinical Aspects of COVID-19; a Narrative Review. *Archives ofAcademic EmergencyMedicine* **8**, 41.
3. Johns Hopkins Coronavirus Resource Center. In press. COVID-19 Map - Johns Hopkins Coronavirus Resource Center. See https://coronavirus.jhu.edu/map.html (accessed on 21 May 2020).
4. Our world in Data. In press. GitHub - owid/covid-19-data: Data on COVID-19 (coronavirus) cases, deaths, hospitalizations, tests • All countries • Updated daily by Our World in Data. See https://github.com/owid/covid-19-data (accessed on 31 March 2022).
5. Centers for Disease Control and Prevention. 2021 COVID Data Tracker, Centers for Disease Control and Prevention. See https://covid.cdc.gov/covid-data-tracker/#datatracker-home (accessed on 31 March 2022).
6. World Health Organization. In press. Coronavirus disease 2019 (COVID-19) Situation Report – 46.
7. World Health Organization. 2020 Laboratory testing strategy recommendations for COVID-19. See https://apps.who.int/iris/bitstream/handle/10665/331509/WHO-COVID-19-lab_testing-2020.1-eng.pdf.
8. World Health Organization (WHO). In press. tracking-SARS-CoV-2-variants. See https://www.who.int/en/activities/tracking-SARS-CoV-2-variants/.
9. Joebges S, Biller-Andorno N. 2020 Ethics guidelines on COVID-19 triage - An emerging international consensus. *Critical Care* **24**, 1–5. (doi:10.1186/s13054-020-02927-1)
10. Yan Bai, MD Lingsheng Yao, MD TaoWei, MD Fei Tian, MD Dong-Yan Jin, PhD Lijuan Chen, PhD MeiyunWang, MD P. 2020 Letters Presumed Asymptomatic Carrier Transmission of COVID-19. (doi:10.1001/jama.2020.2565)
11. Al-Sadeq DW, Nasrallah GK. 2020 The incidence of the novel coronavirus SARS-CoV-2 among asymptomatic patients: A systematic review. *International Journal of Infectious Diseases* **98**, 372–380. (doi:10.1016/j.ijid.2020.06.098)
12. Mallett S *et al.* 2020 At what times during infection is SARS- CoV-2 detectable and no longer detectable using RT-PCR-based tests? A systematic review of individual participant data. *BMC Med* **18**, 1–17. (doi:doi:10.1186/s12916-020-01810-8)
13. Yukari C. Manabe M, Joshua S. Sharfstein M, Katrina Armstrong M. 2020 The Need for

medRxiv preprint doi: https://doi.org/10.1101/2021.08.31.21262868; this version posted July 15, 2022. The copyright holder for this preprint (which was not certified by peer review) is the author/funder, who has granted medRxiv a license to display the preprint in perpetuity. It is made available under a CC-BY-NC-ND 4.0 International license .

More and Better Testing for COVID-19. (doi:10.1001/jama.2020.21694)

14. Rhee C, Kanjilal S, Baker M, Klompas M. 2021 Duration of Severe Acute Respiratory Syndrome Coronavirus 2 (SARS-CoV-2) Infectivity: When Is It Safe to Discontinue Isolation? *Clinical Infectious Diseases* **72**, 1467–1474. (doi:10.1093/cid/ciaa1249)
15. Wilson E, Donovan C v, Campbell M. 2020 Multiple COVID-19 Clusters on a University Campus —. *MMWR Morb Mortal Wkly Rep* **69**, 1416–1418.
16. Id VB, Mallein B. 2021 Group testing as a strategy for COVID-19 epidemiological monitoring and community surveillance. *PLoS Computational Biology* **17**, 1–25. (doi:10.1371/journal.pcbi.1008726)
17. Organisation for Economic Cooperation and Development. 2020 Testing for COVID-19: A way to lift confinement restrictions. See https://read.oecd-ilibrary.org/view/?ref=129_129658-l62d7lr66u&title=Testing-for-COVID-19-A-way-to-lift-confinement-restrictions.
18. Signorini SG, Brugnoni D. 2021 Less is more : an ecological and economic point of view on appropriate use of lab testing for COVID patients. *Bioanalysis* , 7–9. (doi:10.4155/bio-2021-0064)
19. Centers for Disease Control and Prevention. 2020 Overview of testing for SARS-CoV-2 (COVID-19). See https://www.cdc.gov/coronavirus/2019-ncov/hcp/testing-overview.html. Accessed 29 August 2020.
20. Id DRB, Bish EK, El-hajj H, Aprahamian H. 2021 A robust pooled testing approach to expand COVID-19 screening capacity. *PLoS ONE* , 1–15. (doi:10.1371/journal.pone.0246285)
21. Japanese society of pediatrics. In press. Thought on COVID-19 testing. See http://www.jpeds.or.jp/modules/activity/index.php?content_id=329 (accessed on 21 May 2020).
22. World Health Organization. In press. WHO Director-General's opening remarks at the media briefing on COVID-19 - 16 March 2020. See https://www.who.int/director-general/speeches/detail/who-director-general-s-opening-remarks-at-the-media-briefing-on-covid-19---16-march-2020 (accessed on 21 May 2020).
23. Godlee F. 2020 The burning building. *The BMJ* **368**, 2020. (doi:10.1136/bmj.m1101)
24. Peto J. 2020 Covid-19 mass testing facilities could end the epidemic rapidly. *The BMJ* **368**, 110110. (doi:10.1136/bmj.m1163)
25. World Health Organization. 2021 COVID-19: Laboratory and diagnosis.
26. Phelan. 2018 Mathematical models to characterize early epidemic growth: A Review Gerardo. *Physiol Behav* **176**, 139–148. (doi:10.1016/j.plrev.2016.07.005.Mathematical)
27. Roguski KM *et al.* 2019 Estimates of global seasonal influenza-associated respiratory mortality: a modelling study. *The Lancet* **391**, 1285–1300. (doi:10.1016/S0140-

medRxiv preprint doi: https://doi.org/10.1101/2021.08.31.21262868; this version posted July 15, 2022. The copyright holder for this preprint (which was not certified by peer review) is the author/funder, who has granted medRxiv a license to display the preprint in perpetuity. It is made available under a CC-BY-NC-ND 4.0 International license .

6736(17)33293-2)

28. Fang Y, Nie Y, Penny M. 2020 Transmission dynamics of the COVID-19 outbreak and effectiveness of government interventions: A data-driven analysis. *J Med Virol* (doi:10.1002/jmv.25750)

29. Tang B, Bragazzi NL, Li Q, Tang S, Xiao Y, Wu J. 2020 An updated estimation of the risk of transmission of the novel coronavirus (2019-nCov). *Infect Dis Model* **5**, 248–255. (doi:10.1016/j.idm.2020.02.001)

30. Kucharski AJ *et al.* 2020 Early dynamics of transmission and control of COVID-19: a mathematical modelling study. *The Lancet Infectious Diseases* **20**, 553–558. (doi:10.1016/S1473-3099(20)30144-4)

31. Backer J, Klinkenberg D, Wallinga J. 2020 The incubation period of 2019-nCoV infections among travellers from Wuhan, China. *Eurosurveillance* , 1–6. (doi:10.1101/2020.01.27.20018986)

32. Bi Q *et al.* 2020 Epidemiology and transmission of COVID-19 in 391 cases and 1286 of their close contacts in Shenzhen, China: a retrospective cohort study. *The Lancet Infectious Diseases* **20**, 911–919. (doi:10.1016/S1473-3099(20)30287-5)

33. Kuniya T. 2020 Prediction of the Epidemic Peak of Coronavirus Disease in Japan, 2020. *J Clin Med* **9**. (doi:10.3390/jcm9030789)

34. Linton NM, Kobayashi T, Yang Y, Hayashi K, Akhmetzhanov AR, Jung SM, Yuan B, Kinoshita R, Nishiura H. 2020 Incubation period and other epidemiological characteristics of 2019 novel coronavirus infections with right truncation: A statistical analysis of publicly available case data. *Journal of Clinical Medicine* **9**, 538. (doi:10.1101/2020.01.26.20018754)

35. Joseph TW, Leung K, Leung GM. 2020 Nowcasting and forecasting the potential domestic and international spread of the 2019-nCoV outbreak originating in Wuhan, China: a modelling study. *The Lancet* **395**, 689–697. (doi:10.1016/S0140-6736(20)30260-9)

36. Iwata K, Miyakoshi C. 2020 A Simulation on Potential Secondary Spread of Novel Coronavirus in an Exported Country Using a Stochastic Epidemic SEIR Model. *Journal of Clinical Medicine* **9**, 944. (doi:10.3390/jcm9040944)

37. Sun H, Qiu Y, Yan H, Huang Y, Zhu Y, Gu J, Chen S. 2021 Tracking Reproductivity of COVID-19 Epidemic in China with Varying Coefficient SIR Model. *Journal of Data Science* **18**, 455–472. (doi:10.6339/jds.202007_18(3).0010)

38. Rocklöv J, Sjödin H, Wilder-Smith A. 2021 COVID-19 outbreak on the diamond princess cruise ship: Estimating the epidemic potential and effectiveness of public health countermeasures. *Journal of Travel Medicine* **27**, 1–7. (doi:10.1093/JTM/TAAA030)

39. Lin L *et al.* 2020 Artificial Intelligence Distinguishes COVID-19 from Community Acquired Pneumonia on Chest CT. *Applied Intelligence* **2019**, 1–5.

medRxiv preprint doi: https://doi.org/10.1101/2021.08.31.21262868; this version posted July 15, 2022. The copyright holder for this preprint (which was not certified by peer review) is the author/funder, who has granted medRxiv a license to display the preprint in perpetuity. It is made available under a CC-BY-NC-ND 4.0 International license .

(doi:10.1148/radiol.2020200905)

40. Roda WC, Varughese MB, Han D, Li MY. 2020 Why is it difficult to accurately predict the COVID-19 epidemic? *Infect Dis Model* **5**, 271–281. (doi:10.1016/j.idm.2020.03.001)

41. World Health Organization. 2020 China Joint Mission on Coronavirus Disease 2019 (COVID-19). *World health organization*. **2019**, 16–24. See https://www.who.int/publications/i/item/report-of-the-who-china-joint-mission-on-coronavirus-disease-2019-(covid-19) (accessed on 21 May 2020).

42. Pulliam JRC, van Schalkwyk C, Govender N, von Gottberg A, Cohen C, Groome MJ, Dushoff J, Mlisana K, Moultrie H. 2022 Increased risk of SARS-CoV-2 reinfection associated with emergence of Omicron in South Africa. *Science (1979)* **376**, 1–43. (doi:10.1126/science.abn4947)

43. GISAID. In press. GISAID - Initiative. See https://www.gisaid.org/ (accessed on 9 May 2021).

44. Shahid Z *et al.* 2020 COVID-19 and Older Adults: What We Know. *J Am Geriatr Soc* **68**, 926–929. (doi:10.1111/jgs.16472)

45. Thomas DM, Sturdivant R, Dhurandhar N v., Debroy S, Clark N. 2020 A Primer on COVID-19 Mathematical Models. *Obesity* **28**, 1375–1377. (doi:10.1002/oby.22881)

46. Sharp TM *et al.* 2021 Antibody Persistence through 6 Months after the Second Dose of mRNA-1273 Vaccine for Covid-19. *New England Journal of Medicine* **384**, 2257–2259. (doi:10.1056/nejmc2023298)

47. Christian HH, Daniela M, Sophie MG, Kåre M, Steen E. 2020 Assessment of protection against reinfection with SARS-CoV-2 among 4 million PCR-tested individuals in Denmark in 2020: a population-level observational study Christian. *The Lancet* , 19–21. (doi:10.1016/ S0140-6736(21)00575-4)

48. United Nations. 2018 The World's Cities in 2018: Data Booklet. (doi:10.18356/C93F4DC6-EN)

49. Ai T, Yang Z, Hou H, Zhan C, Chen C, Lv W, Tao Q, Sun Z, Xia L. 2020 Correlation of Chest CT and RT-PCR Testing in Coronavirus Disease 2019 (COVID-19) in China: A Report of 1014 Cases. *Radiology* , 200642. (doi:10.1148/radiol.2020200642)

50. Long C *et al.* 2020 Diagnosis of the Coronavirus disease (COVID-19): rRT-PCR or CT? *European Journal of Radiology* **126**. (doi:10.1016/j.erad.2020.108961)

51. Lai S *et al.* 2021 Effect of non-pharmaceutical interventions to contain COVID-19 in China. *Natutre* **585**, 410–413. (doi:10.1038/s41586-020-2293-x.Effect)

medRxiv preprint doi: https://doi.org/10.1101/2021.08.31.21262868; this version posted July 15, 2022. The copyright holder for this preprint (which was not certified by peer review) is the author/funder, who has granted medRxiv a license to display the preprint in perpetuity. It is made available under a CC-BY-NC-ND 4.0 International license .

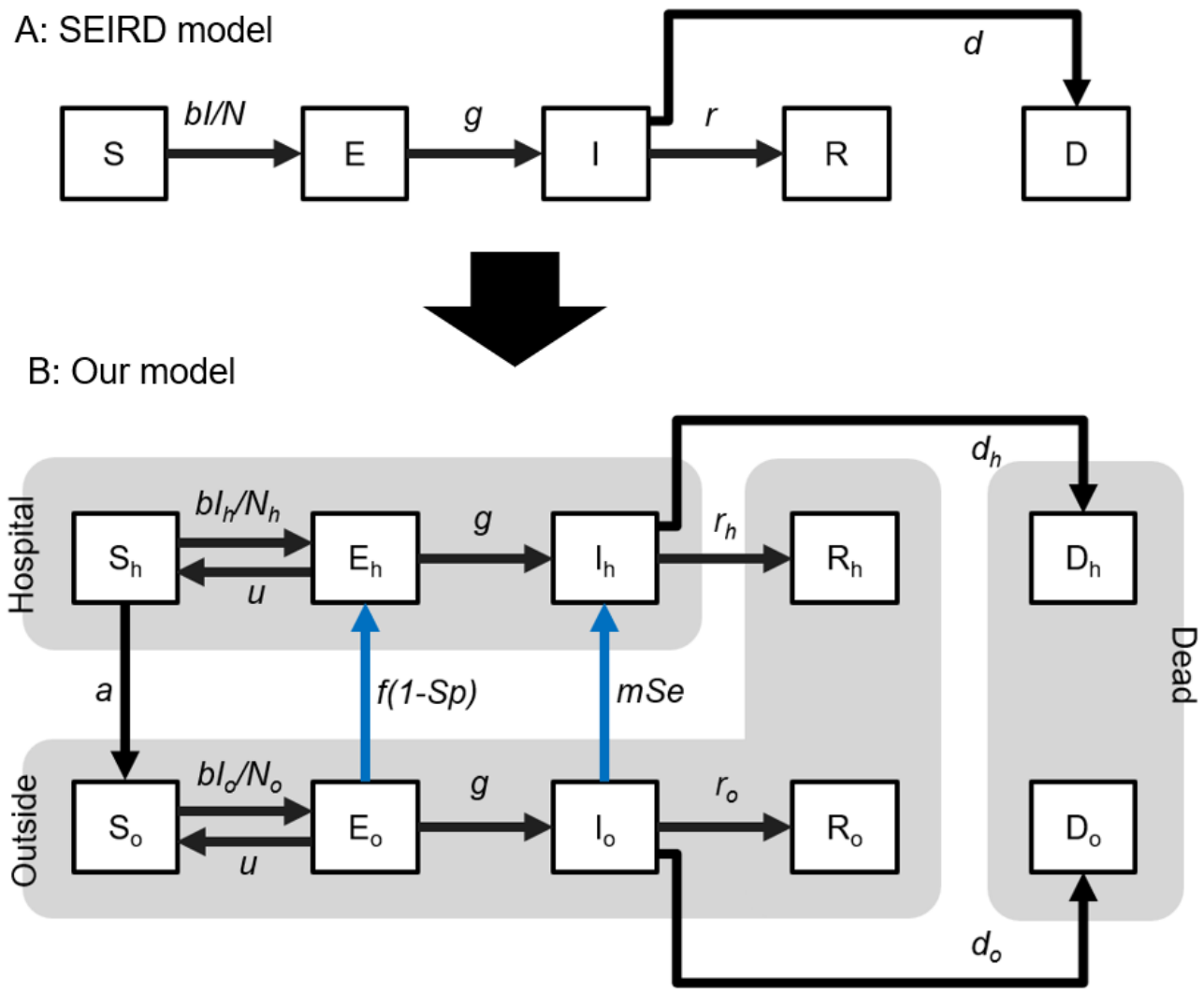

Figure 1: Classical SEIRD and testing-SEIRD models

(A) Classical SEIRD model: Susceptible population 'S' is exposed by infectious population 'I' at a rate proportional to the fraction of the infectious population. The exposed population 'E' become infectious 'I'. The infected population finally recovers 'R' or become dead 'D'. (B) Testing-SEIRD model: The population is divided into two subpopulations; inside and outside hospitals. The exposed 'E_o' and infectious population outside 'I_o' are hospitalised if evaluated as positive by testing. Susceptible population 'S_h' is left from the hospitals. The black lines indicate the transitions of populations, regardless of capacity effect. The blue lines indicate the transitions of the populations, considering the capacity effect. Transitions from both 'E_o' to 'E_h' and 'I_o' to 'I_h' are determined as hospitalised.

medRxiv preprint doi: https://doi.org/10.1101/2021.08.31.21262868; this version posted July 15, 2022. The copyright holder for this preprint (which was not certified by peer review) is the author/funder, who has granted medRxiv a license to display the preprint in perpetuity. It is made available under a CC-BY-NC-ND 4.0 International license .

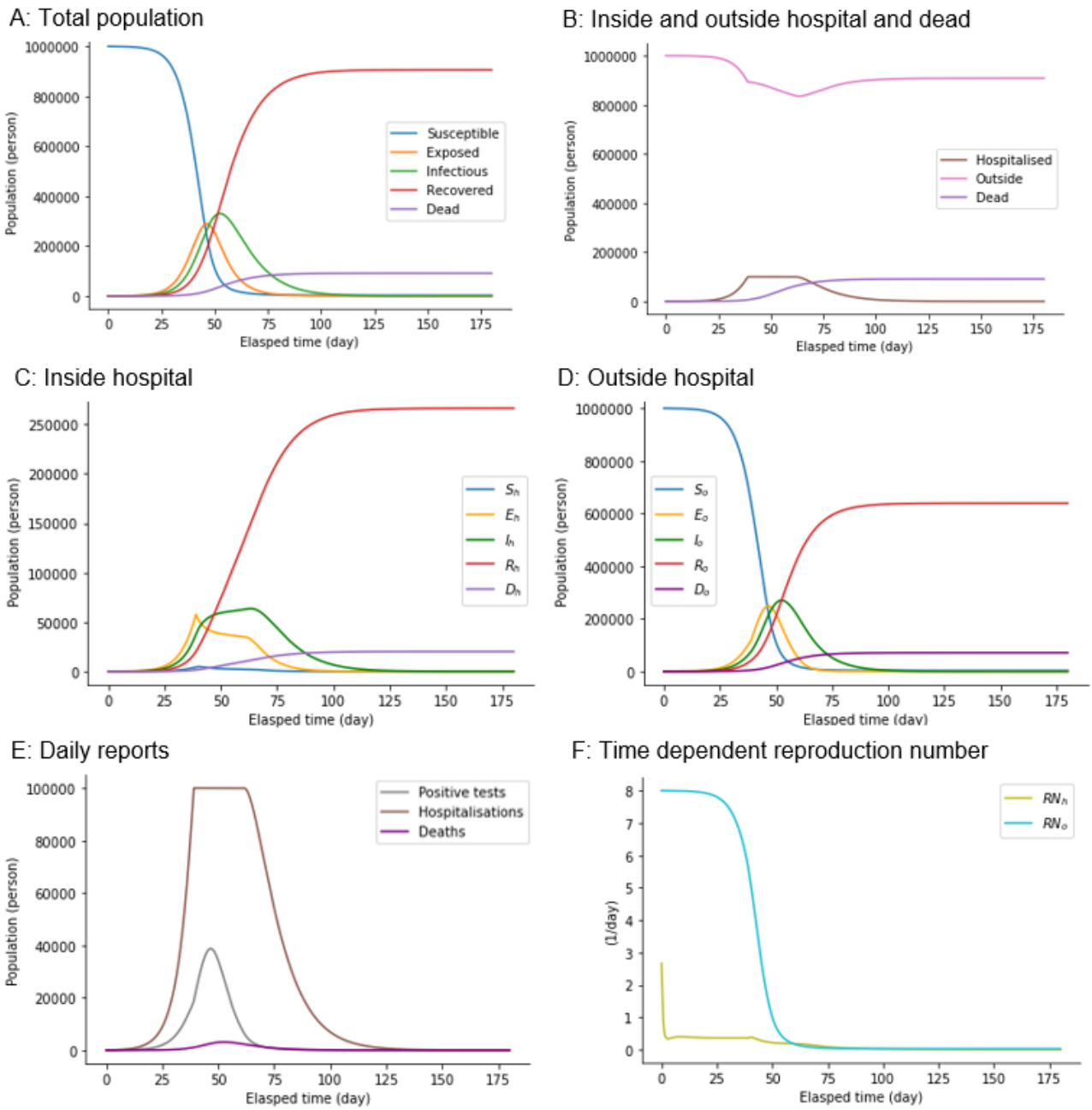

Figure 2: Changes in components over time in the testing-SEIRD model

Time-courses of (A) populations of all infectious states, irrespective of being inside and outside hospitals; (B) Populations inside and outside hospitals and dead populations, irrespective of infectious states; (C) Populations of all infectious states inside hospitals; (D) Populations of all infectious states outside hospitals; (E) Daily reports of positive tests, hospitalisations, and deaths; (F) Time-courses of reproduction numbers inside and outside hospitals, as described in Materials and Methods section.

medRxiv preprint doi: https://doi.org/10.1101/2021.08.31.21262868; this version posted July 15, 2022. The copyright holder for this preprint (which was not certified by peer review) is the author/funder, who has granted medRxiv a license to display the preprint in perpetuity. It is made available under a CC-BY-NC-ND 4.0 International license .

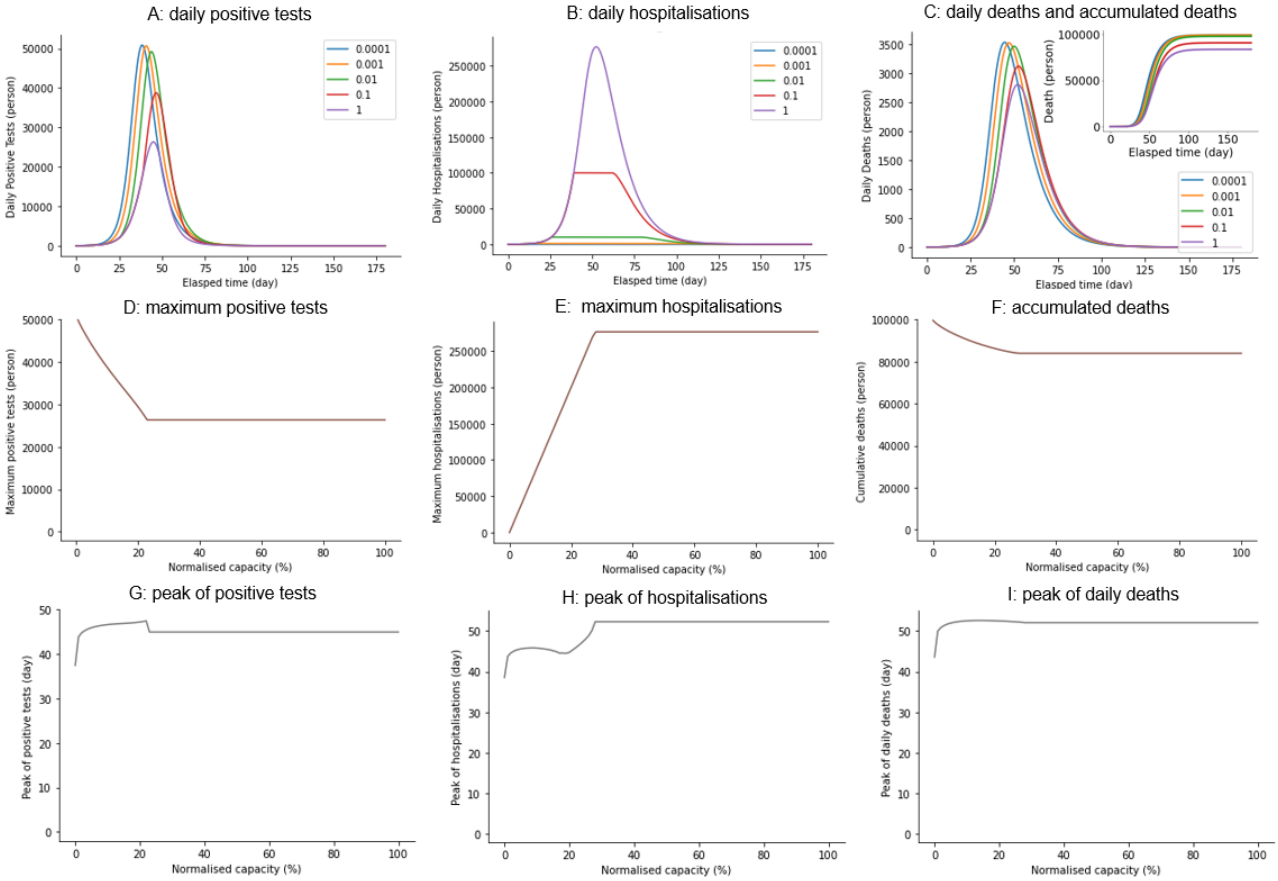

Figure 3: Impact of hospitalisations capacity on the three variables

Time courses of (A) Daily reports of positive tests; (B) Daily reports of hospitalisations; (C) Daily reports of deaths with varying hospitalisation capacity. C/N indicates the capacity normalised to the total population. Hospitalisation capacity dependencies of (D) Maximum positive reports; (E) Maximum hospitalisations; (F) Cumulative deaths. Hospitalisation capacity-dependencies of (G) Peaks of daily reports of positive tests; (H) Peaks of hospitalisations; (I) Peaks of daily deaths.

medRxiv preprint doi: https://doi.org/10.1101/2021.08.31.21262868; this version posted July 15, 2022. The copyright holder for this preprint (which was not certified by peer review) is the author/funder, who has granted medRxiv a license to display the preprint in perpetuity. It is made available under a CC-BY-NC-ND 4.0 International license .

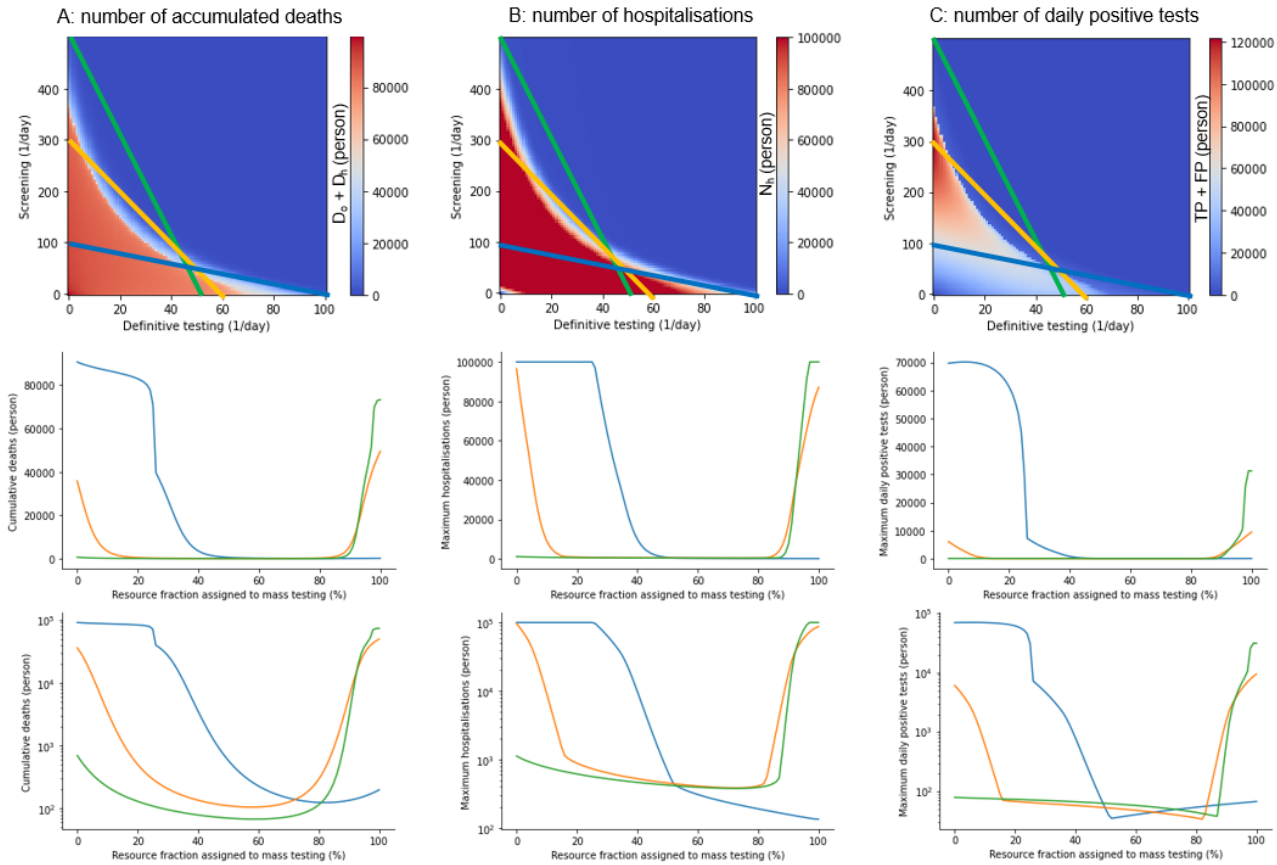

Figure 4: Infectious spread based on the testing strategy

The upper panels represent the number of (A) cumulative deaths, (B) maximum hospitalizations, and (C) maximum daily positive tests depending on the rates of follow-up and mass-testing. The three lines in these heatmaps represent the possible testing strategies subject to different total resource for testing with different ratios for the testing costs. The middle panels represent the numbers along the three lines in the heatmaps. The lower panels represent semilog-plots of the middle panels. L=500, c_f =1, c_m =10 in the green line, L=300, c_f =1, c_m =5 in the blue line, and L=100, c_f =1, c_m =1 in the orange line.

medRxiv preprint doi: https://doi.org/10.1101/2021.08.31.21262868; this version posted July 15, 2022. The copyright holder for this preprint (which was not certified by peer review) is the author/funder, who has granted medRxiv a license to display the preprint in perpetuity. It is made available under a CC-BY-NC-ND 4.0 International license .

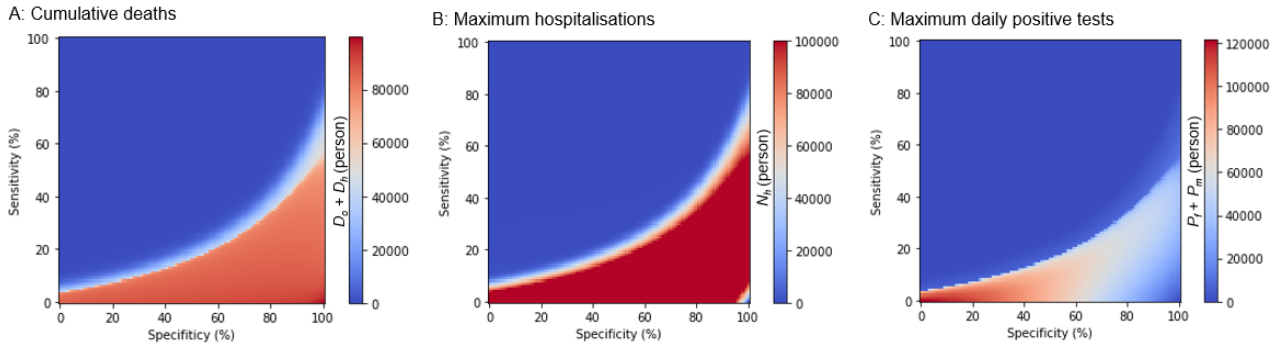

Figure 5: Infectious spread based on the testing properties

Number of (A) Cumulative deaths, (B) Maximum hospitalisations, and (C) Maximum daily positive tests based on the sensitivity and specificity of the testing.

medRxiv preprint doi: https://doi.org/10.1101/2021.08.31.21262868; this version posted July 15, 2022. The copyright holder for this preprint (which was not certified by peer review) is the author/funder, who has granted medRxiv a license to display the preprint in perpetuity. It is made available under a CC-BY-NC-ND 4.0 International license .

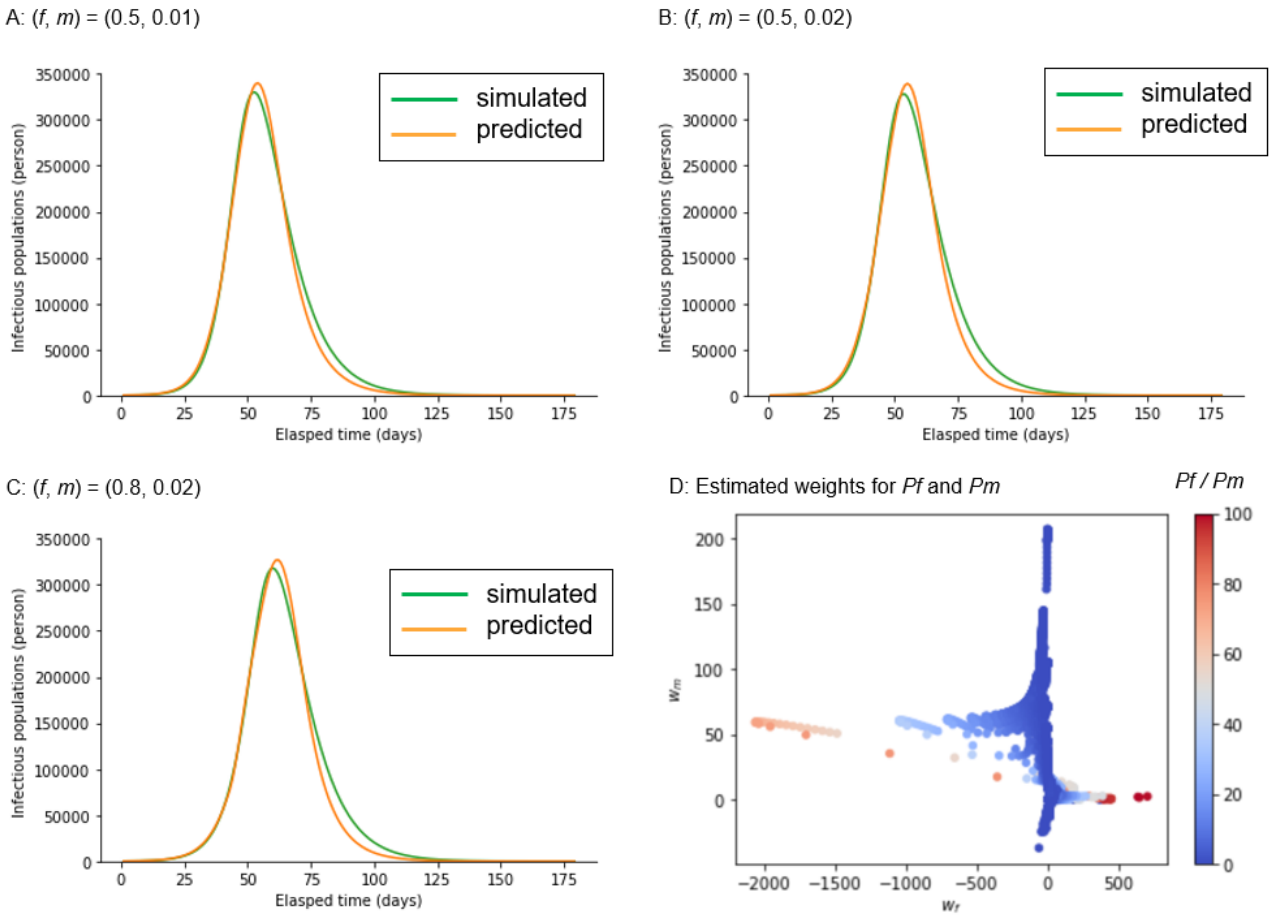

Figure 6: Prediction of infectious population from daily reports of positive tests

(A-C) The Green and orange lines indicate the simulated and predicted infectious populations (I_h and I_o) with different testing strategies. The infectious populations are estimated by the linear regression *as* $w_f P_f + w_m P_m$, where w_f and w_m indicate the weights and P_f and P_m indicate the daily positive reports of follow-up and mass-testing, namely f (1-Sp) and mSe, respectively. The weights are estimated by the least square method. (D) The estimated weights for P_f and P_m are plotted, considering various combinations of ratios of the follow-up cost to the mass-testing cost (P_f/P_m).

medRxiv preprint doi: https://doi.org/10.1101/2021.08.31.21262868; this version posted July 15, 2022. The copyright holder for this preprint (which was not certified by peer review) is the author/funder, who has granted medRxiv a license to display the preprint in perpetuity. It is made available under a CC-BY-NC-ND 4.0 International license .

A

Variable	Value
S_h, E_h, I_h	1
I_o	97
S_o	999900
E_o, R_h, R_o, D_h, D_o	0

Parameter	Value
Se	0.7
Sp	0.7
f	0.05
m	0.01
b	1
u	0.04
g	0.16
r_h	0.093
r_o	0.096
d_h	0.007
d_o	0.01

B

Mode of test	*Se*	*Sp*
CT	0.98[28], 0.97[39,50], 0.8 to 0.9[51], 0.972[52]	0.828 to 0.96[51]
PCR	0.71[28], 0.846[52]	n/a

C

Reference	Model	*b*	*g*	r_h	r_o	d_h	d_o
Fang[28]	eSEIR	0.9 e-5 to e-6†	0.143	0.056	n/a	n/a	n/a
Tang[29]	n/a	2.1 e-8	0.126	n/a	0.14	1.78 e-5	n/a
Kucharski[30]	eSEIR	n/a	0.156	n/a	n/a	n/a	n/a
Backer[31]	n/a	n/a	0.143 to 0.33	n/a	n/a	n/a	n/a
Bi Q[32]	n/a	n/a	n/a	n/a	n/a	n/a	n/a
Kuniya[33]	SEIR	0.2 e-8†	n/a	n/a	n/a	n/a	n/a
Linton[34]	n/a	n/a	0.2	n/a	n/a	n/a	n/a
Iwata[36]	SEIR	n/a	0.167 to 0.208	0.13 to 0.417	n/a	n/a	n/a
Sun[37]	vSIR	n/a	n/a	0.1	n/a	n/a	n/a
Rocklöv[38]	SEIR	0.4 e-4 or 0.12 e-4†	0.2	n/a	n/a	n/a	n/a
Roda[40]	SIR/SEIR	8.68 e-8	0.631	0.1	n/a	n/a	n/a

D

Reference	Incubation period	Infectious period
Kucharski[30]	5.2	2.9
Backer[31]	6.5	n/a
Bi Q[32]	4.8	1.5
Wu[35]	6.1	2.3
Rocklöv[38]	5	10
Lin[39]	5.2	2.3
WHO-China Joint[41]	5.5	n/a

Table 1: Variables and parameters in reports during the early stage of pandemic

(A) Initial values for variables and parameters and (B) Reported sensitivity and specificity of PCR and CT for detecting COVID-19. Cells expressed as n/a indicate that we cannot find the (C) reported transition parameters with models. Values with † are calculated from the original values for comparison. All the values have dimensions of [one/day]. We cannot find values or models for the cells expressed as n/a. The values with † equal original values divided by the total population involved. (D) Reported incubation period and infectious period. All values have dimensions of [day].

medRxiv preprint doi: https://doi.org/10.1101/2021.08.31.21262868; this version posted July 15, 2022. The copyright holder for this preprint (which was not certified by peer review) is the author/funder, who has granted medRxiv a license to display the preprint in perpetuity. It is made available under a CC-BY-NC-ND 4.0 International license .

Supplementary Figures

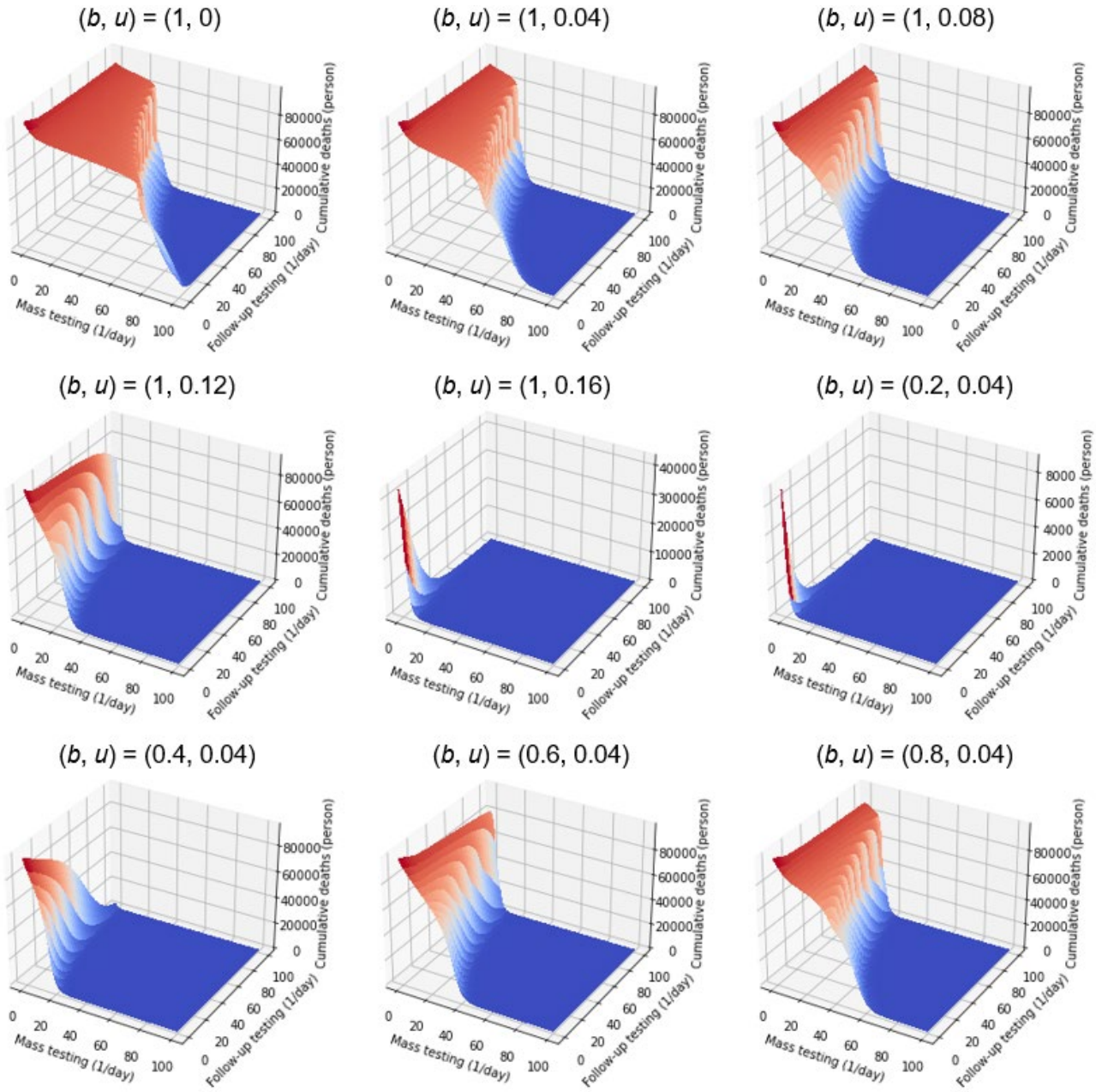

Figure S1: Sensitivity analyses of parameters *b* and *u* on the number of cumulative deaths

Simulations were performed with different values of *b* and *u*.

medRxiv preprint doi: https://doi.org/10.1101/2021.08.31.21262868; this version posted July 15, 2022. The copyright holder for this preprint (which was not certified by peer review) is the author/funder, who has granted medRxiv a license to display the preprint in perpetuity. It is made available under a CC-BY-NC-ND 4.0 International license .

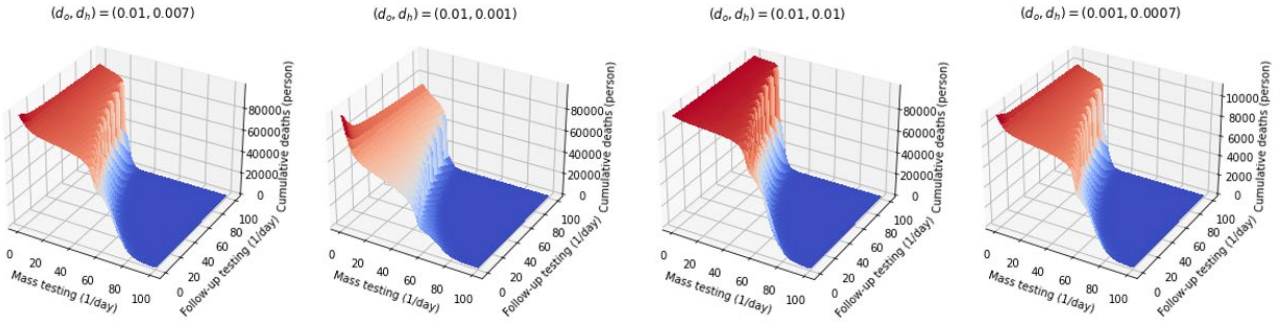

Figure S2: Sensitivity analyses of d_o and d_h on the number of cumulative deaths

Simulations were performed with different values of d_o, d_h, where (d_o, d_h) of (0.01, 0.007) is a reference standard, (0.01, 0.001) means advance in treatment, (0.01, 0.01) means futile treatment, and (0.001, 0.0007) means reduction in overall mortality.

medRxiv preprint doi: https://doi.org/10.1101/2021.08.31.21262868; this version posted July 15, 2022. The copyright holder for this preprint (which was not certified by peer review) is the author/funder, who has granted medRxiv a license to display the preprint in perpetuity. It is made available under a CC-BY-NC-ND 4.0 International license .

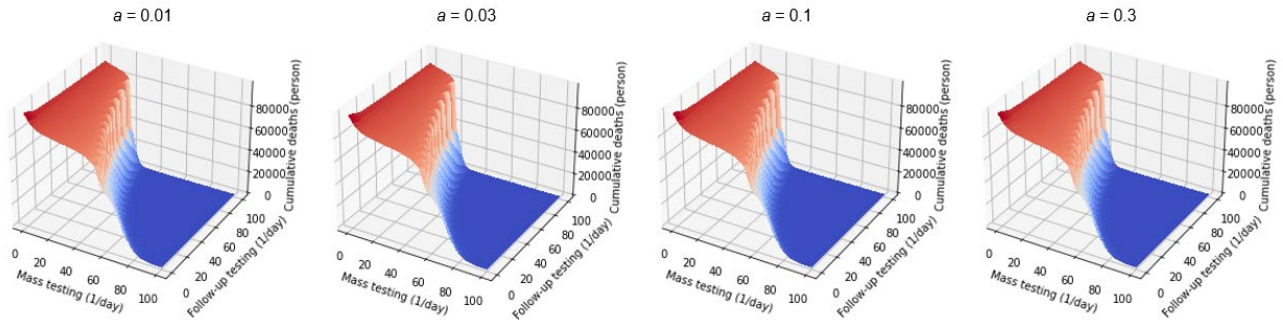

Figure S3: Sensitivity analyses of parameter *a* on the number of cumulative deaths

Simulations were performed with different values of parameter *a*.